Guilu Erxian oral liquid mitigates oxidative damage in spermatogonial cells *via* miR-6739-5p modulation and PI3K/AKT pathway activation: a functional histocytochemical study

Zefeng Sun,[1] Xinrong Fan,[2] Zhenquan Liu[1]

[1]Beijing University of Chinese Medicine, Beijing; [2]China Academy of Chinese Medical Science, Beijing, China

ABSTRACT

Oxidative stress is a major contributor to male infertility, particularly oligoasthenozoospermia. This study aimed to investigate the cytoprotective mechanism of Guilu Erxian oral liquid (GLEX) against H_2O_2-induced oxidative damage in spermatogonial cells, focusing on miR-6739-5p regulation and activation of the PI3K/AKT pathway using histocytochemical approaches. An oxidative stress model was established in rat spermatogonial stem cells (SSCs) with 250 μM H_2O_2. Cell proliferation, apoptosis, reactive oxygen species (ROS) accumulation, and DNA oxidative damage were assessed using EdU incorporation, flow cytometry, immunofluorescence, and 8-hydroxy-2'-deoxyguanosine (8-OHdG) ELISA. Expression of miR-6739-5p and phosphatidylinositol 3-kinase/protein kinase B (PI3K/AKT) pathway components (*PIK3CA*, p-PI3K, p-AKT) was evaluated by RT-qPCR and Western blotting. The interaction between miR-6739-5p and *PIK3CA* was confirmed *via* dual-luciferase reporter assay. The cytoprotective effects of GLEX were examined through pre-treatment and quantified using histochemical and cytological markers. H_2O_2 treatment significantly impaired cell viability, increased apoptosis and ROS production, and upregulated miR-6739-5p. Overexpression of miR-6739-5p exacerbated damage, while silencing reversed it and restored PI3K/AKT signaling. GLEX pretreatment effectively reduced miR-6739-5p expression, restored cell viability, suppressed oxidative and inflammatory markers (ROS, 8-OHdG, TNF-α, IL-1β), and enhanced PI3K/AKT activation. These effects were comparable to PI3K pathway activation. GLEX confers histocytochemical protection to spermatogonial cells under oxidative stress by downregulating miR-6739-5p and activating the PI3K/AKT pathway. This study highlights a novel regulatory mechanism and supports GLEX as a potential therapeutic agent for oxidative stress-associated male infertility.

Key words: Guilu Erxian; spermatogonial cells; histochemistry; oxidative stress; miR-6739-5p; PI3K/AKT pathway.

Correspondence: Zhenquan Liu, MD. Beijing University of Chinese Medicine, No. 11, Bei San Huan Dong Lu, Chaoyang District, Beijing 100029, China. E-mail: lzqbzy@sina.com

Contributions: all the authors made a substantive intellectual contribution, read and approved the final version of the manuscript and agreed to be accountable for all aspects of the work.

Conflict of interest: the authors declare no competing interest, and all authors confirm accuracy.

Availability of data and materials: the datasets used and/or analyzed during the current study are available upon reasonable request from the corresponding author.

Introduction

Infertility has become a prominent global reproductive health issue. Around the world, approximately 10% to 15% of couples in their reproductive years are struggling with infertility, with male factors accounting for roughly 50% of these cases.[1] Male infertility can be influenced by a variety of factors.[2] In recent years, oxidative stress has risen to prominence as one of the leading causes of male infertility, largely due to shifts in environmental and lifestyle conditions.[3] Research indicates that elevated levels of oxidative stress can induce DNA damage and compromise the viability of reproductive cells. In extreme cases, this can result in conditions like azoospermia (the complete lack of sperm in semen) and oligozoospermia (a low sperm count).[4] It is worth noting that azoospermia, which is frequently accompanied by decreased sperm motility, affects 40% of infertile men.[5] Since the pathogenesis of oligozoospermia and other types of male infertility is intricately linked to disruptions at different stages of spermatogenesis, including spermatogonial cell replication, meiosis, and spermiogenesis,[6] there is a pressing need for further investigation into the pathogenesis of oligozoospermia and male infertility at the level of spermatogonial cells.

Recent research has revealed that microRNAs (miRNAs) - small, single-stranded non-coding RNA molecules- are widely distributed across all human tissues, with a particularly significant presence in the reproductive system.[7] This discovery suggests that miRNAs play a crucial role in male reproductive processes.[8] Studies have identified distinct differences in miRNA expression profiles between healthy men and those diagnosed with oligozoospermia. Notably, significantly higher levels of miR-6739-5p have been observed in the semen of oligozoospermic men, and this upregulation is strongly correlated with the phosphatidylinositol 3-kinase/protein kinase B (PI3K/AKT) pathway and oxidative stress.[9] The PI3K/AKT pathway is well-known for its regulatory effects on spermatogonial cell activity. For example, melatonin has been shown to enhance spermatogonial cell activity by activating the PI3K/AKT signaling pathway, which is achieved through promoting m6A deposition mediated by KIAA-1429.[10] Therefore, exploring the relationship among spermatogonial cells, the miR-6739-5p/PI3K/AKT axis, and oxidative stress is of immense value. It not only aids in clarifying the regulatory mechanisms of spermatogonial cells but also offers promising avenues for the prevention and treatment of male infertility.

In Western medicine, the array of treatment modalities for oligoasthenozoospermia includes testosterone, gonadotropins, corticosteroids, follicle-stimulating hormone, and antioxidants. Systematic reviews indicate that while some treatment strategies produce positive results, others do not.[1] Recently, there has been a burgeoning interest in traditional Chinese medicine (TCM) as a potential therapeutic alternative. With a history stretching back over 2,000 years, TCM has been widely utilized in clinical practice.[12] A meta-analysis of randomized controlled trials has demonstrated that Wuzi Yanzong pill, a traditional Chinese herbal formula, can reduce DNA damage in patients with oligoasthenozoospermia and improve sperm concentration, motility, and acrosomal enzyme activity.[13] Guilu Erxian oral liquid (GLEX), a TCM formulation comprising tortoise shell, deer antler, codonopsis root, and wolfberry, is commonly used in folk medicine for the treatment of oligoasthenozoospermia. Clinical findings within the TCM field suggest that Guilu Erxian paste offers significant therapeutic advantages for patients with oligoasthenozoospermia resulting from kidney deficiency. Notably, the therapeutic effects of this paste persist long after discontinuation of the medication, providing a unique advantage in maintaining a favorable clinical outcome. Moreover, it exhibits an excellent safety profile.[14] In addition, research has shown that GLEX can ameliorate oligoasthenozoospermia induced by *Tripterygium wilfordii* glycosides in rats through the Keap1/Nrf2/GPX4 signaling pathway.[15] However, as of yet, there have been no reports suggesting the involvement of the PI3K/AKT pathway, which serves as an upstream regulator of Nrf2 in this specific process.

Building upon this established foundation, the present study is designed to utilize H_2O_2 to induce oxidative damage in rat spermatogonial stem cells (SSCs), thereby creating an oxidative damage model.[16] The overarching goal is to determine whether miR-6739-5p exhibits distinct expression patterns under these oxidative stress conditions. Subsequently, we intend to clarify the effects of both overexpressing and knocking down miR-6739-5p within the context of this oxidative damage model. Following these preliminary investigations, we will conduct separate explorations into the therapeutic potential and regulatory mechanisms of GLEX and inhibitors of the PI3K/AKT pathway in the oxidative damage model. Our experimental results are expected to reveal that GLEX has the ability to downregulate the expression of miR-6739-5p. This downregulation is likely to set off a chain reaction, activating the PI3K/AKT signaling pathway and, in turn, effectively alleviating the H_2O_2-induced damage to spermatogonial cells. In essence, the therapeutic efficacy of GLEX can be ascribed to its capacity to reduce miR-6739-5p levels, which subsequently initiates the activation of the PI3K/AKT signaling cascade. This groundbreaking discovery provides novel insights into the clinical application of GLEX for the treatment of disorders characterized by oxidative stress-mediated damage in spermatogonial cells, with a particular focus on male infertility associated with oligospermia.

Materials and Methods

Experimental reagents

In this study, a comprehensive array of reagents and kits was utilized. For cell culture and general purposes, we employed rat spermatogonial stem cell complete culture medium (CM-R171, sourced from Procell in Wuhan, China), trypsin (R001100, Gibco, Rockville, MD, USA), cell freezing solution (C0210B-50 mL, Beyotime, Shanghai, China), PBS buffer solution (C0221A, Beyotime), and methanol (HB05, Guangzhou Chemical Reagent, Guangzhou, China) which served as an organic solvent.

When it came to RNA and complementary DNA (cDNA) synthesis, we used the Cell/Tissue Total RNA Isolation Kit V2 (RC112, Vazyme, Nanjing, China), HiScript III 1st Strand cDNA Synthesis Kit (R312, Vazyme), and Taq Pro Universal SYBR qPCR Master Mix (Q712, Vazyme). Primers were obtained from Sangon (Shanghai, China), while hsa-miR-6739-5p mimics and its negative control (NC) were sourced from Guangzhou RiboBio Co., Ltd. (Guangzhou, China). For protein extraction and Western blotting, a variety of reagents were involved. These included APS (ST005, Beyotime), RIPA lysis buffer (P0013B, Beyotime), PMSF (ST506, Beyotime), TEMED (ST728, Beyotime), 30% Acr/Bic (BL513A, Beyotime), Tris-Base (BS083, Biosharp, Hefei, China), TBS buffer powder (BL602A, Beyotime), BSA protein standard (BL673A, Beyotime), Tween-20 (BS100, Biosharp), SDS (3250, BioFroxx, Shanghai, China), Glycine (1275, BioFroxx), skim milk (1172, BioFroxx), BCA protein content determination kit (WB6501, NCM Biotech), 5x SDS-PAGE loading buffer (WB2001, NCM Biotech), and ECL luminescent liquid AB solution (P2100, NCM Biotech). Additionally, Prestained Protein Marker II (G2058-250UL, Servicebio, Wuhan, China) and several antibodies were used for protein detection, namely Recombinant Anti-PI 3 Kinase catalytic subunit alpha/*PIK3CA* antibody

[EPR19693] (ab183957, Abcam, Cambridge, UK), Anti-AKT (phospho T308) antibody (ab38449, Abcam), Recombinant Anti-Nrf2 antibody [EP1808Y] (ab62352, Abcam), Anti-GAPDH antibody [6C5]-Loading Control (ab8245, Abcam), and Phospho-PI3K p85 alpha (Tyr607) Polyclonal Antibody (Thermo Fisher Scientific, Waltham, MA, USA).

In the realm of immunofluorescence and staining, we utilized Triton X-100 (P0096, Beyotime), 4% paraformaldehyde (P0099-500mL, Beyotime), DAPI (C1006, Beyotime), PI dye (ST512, Beyotime), and 10% blocking goat serum (C01-03001, Bioss, Wuhan, China). For cell proliferation and reporter assays, the CCK8 cell proliferation detection kit (BA00208, Beyotime) and Dual-Luciferase Reporter Gene Detection Kit (RG027, Beyotime) were employed.

Finally, for ELISA-based analyses, we used the 8-OHdG ELISA Kit (E-EL-0028, Elabscience, Wuhan, China), Rat Tumor necrosis factor α (TNF-α) ELISA Kit (CB11057-Ra, Coibo, Shanghai, China), and Rat IL-1β ELISA Kit (PI303, Beyotime).

Experimental instruments

The ultra-low temperature freezer utilized in our experiments is manufactured by Haier (Qingdao, China). Our optical microscope is sourced from Shanghai Optical Instrument Factory No. 1. For cell culture applications, we employ a CO_2 incubator, a laminar flow hood, and a constant-temperature water bath, all supplied by Shanghai Boxun Industrial & Medical Equipment Co., Ltd. The XUEKE-IMS-150 laboratory ice maker, essential for maintaining low temperatures in specific experiments, is produced by Tuohe Electromechanical Technology (Shanghai) Co., Ltd. Our liquid nitrogen tank (model YDS-175-276) is obtained from Huate Gas Company, while the CENTRA pure water system, provided by ELGA Veolia Water Treatment Technologies (Shanghai) Co., Ltd., meets our ultrapure water requirements. In molecular biology workflows, we use the CFX96 Touch 1855195 real-time fluorescence quantitative PCR instrument (Bio-Rad Laboratories, Hercules, CA, USA) alongside a Western blotting system comprising a Criterion™ electrophoresis cell and a Trans-Blot® transfer tank (both Bio-Rad). Additionally, a general PCR instrument from BIOER Company supports our nucleic acid amplification needs. For shaking and mixing tasks, we utilize the Orbital Shaker TS-100 (Qilin Beier [Kylin-Bell] Instrument Manufacturing Co., Ltd., Haimen, China). The JP-K6000 chemiluminescence analyzer (Jiapeng Technology Co., Ltd., Shanghai, China) detects luminescent signals, while the RT-6000 microplate reader (Rayto Life and Analytical Sciences Co., Ltd., Shenzhen, China) facilitates high-throughput absorbance/fluorescence measurements.

Cell culture and grouping

SSCs were obtained from Wuhan Procell Life Science & Technology Co., Ltd. (Wuhan, China). These cells were cultured in a specialized complete medium optimized for SSC maintenance at 37°C with 9 relative humidity in a CO_2 incubator (5% CO_2). Upon reaching 80-90% confluence, the spent medium was aspirated, and the cells were gently washed twice with 2 mL of phosphate-buffered saline (PBS). Subsequently, 2 mL of a digestion solution (0.25% trypsin/0.02% EDTA) was added, and the cells were monitored microscopically for ~1 min until they adopted a rounded morphology. Digestion was terminated by adding 6 mL of complete medium, followed by gentle pipetting to detach and collect the cells. After centrifugation at 800 rpm for 5 min at 4°C, the supernatant was discarded, and the cell pellet was resuspended in fresh medium. The cells were then either passaged or counted and seeded according to experimental requirements.

Part 1: to investigate the expression pattern of hsa-miR-6739-5p in spermatogonial cells subjected to oxidative stress, the specific experimental groupings are detailed in Table 1.

Part 2: to validate the impact of hsa-miR-6739-5p on oxidative stress-induced damage in spermatogonial cells *via* the PI3K/AKT signaling pathway, the experimental design is outlined in Table 2, with the mutation site specified in Table 3.

Part 3: to explore the protective effects of GLEX against oxidative stress-induced damage in spermatogonial cells through modulation of hsa-miR-6739-5p and the PI3K/AKT pathway, the specific groupings are presented in Table 4. In this study, a double-blind randomized design was employed to allocate cells into distinct experimental groups. Throughout the experimental process, researchers remained blinded to group assignments until data processing was finalized, which occurred only after cells in each group had been treated with the respective positive control drugs and experimental agents. The blind was broken exclusively at this stage. This methodology was implemented to eliminate potential subjective bias and ensure experimental rigor.

EdU assay for cell proliferation

Cells in the logarithmic growth phase were seeded at a density of 1×10^6 cells per well in 6-well plates and subjected to treatments according to the experimental group assignments. Initially, a 2× working solution of EdU was prepared. An equal volume of preheated 2× EdU solution (20 μM) was then added to each well to achieve a final concentration of 1× EdU (10 μM), and the cells were incubated at 37°C for an additional 2 h. Following EdU labeling, the culture medium was aspirated, and each well was supplemented with 1 mL of fixative solution (4% paraformaldehyde in PBS) for fixation at room temperature (RT) for 15 min. The cells were subsequently washed three times with wash buffer (PBS), with each wash lasting 3-5 min. To enhance membrane permeability, the plates were treated with permeabilization buffer (0.3% Triton X-100 in PBS) at RT for 15 min, followed by two additional washes with PBS (5 min each).

To prepare the Click Additive Solution, one vial of Click Additive was dissolved in 1.3 mL of deionized water and mixed thoroughly until completely solubilized. Following removal of the wash buffer from the previous step, 0.5 mL of the Click reaction mixture was added to each well. The culture plate was gently agitated to ensure uniform distribution of the reaction mixture across the samples, then incubated at room temperature (RT) in the dark for 30 min. After aspirating the Click reaction mixture, the wells were washed three times with PBS-based wash buffer (5 min per wash). Subsequently, 1 mL of DAPI staining solution (1 μg/mL in PBS) was added to each well and incubated for 5 min to counterstain nuclei, followed by three additional washes with PBS (5 min each). Microscopic observations were performed using a Keyence BZ-H4XD fluorescence microscope (Keyence Co., Osaka, Japan) equipped with a 10× eyepiece and 20× objective lens. Detection parameters were set as follows: DAPI (Ex: 360/40 nm, Em: 460/50 nm) and EdU-488 (Ex: 470/40 nm, Em: 520/50 nm). Random fields of view were systematically selected, imaged, and documented. During DNA synthesis, the thymidine deoxynucleoside analog EdU incorporates into newly synthesized DNA and is subsequently conjugated to Alexa Fluor 488 *via* a copper-catalyzed click chemistry reaction. Quantitative analysis was performed by

Table 1. Experimental grouping for part 1.

Grouping	Specific procedures
SSCs	Normal culturing
SSCs+H_2O_2	Treatment with 250 μmol/L for 2 h 15

calculating the EdU positivity rate, defined as the percentage of EdU-positive cells (green fluorescence) relative to total DAPI-stained nuclei. To ensure experimental reproducibility, all procedures were performed in triplicate.

CCK-8 assay for cell viability

Cells in the logarithmic growth phase were seeded into a 96-well plate at a density of 2,000 cells per well and incubated for 4-8 h to ensure firm adhesion to the plate surface. Upon confirmation of cell attachment, varying concentrations of CURNPs were added to each well according to predefined experimental groups, with each group containing six replicate wells to ensure statistical robustness. The cells were then incubated for an additional 24 h. Two hours prior to the end of the incubation period, 10 μL of CCK-8 solution was gently added to each well to evaluate cell viability. Following incubation, absorbance at 450 nm was measured using a microplate reader, providing a quantitative assessment of cell proliferation or cytotoxicity. To ensure experimental reproducibility, all procedures were performed in triplicate.

Measurement of reactive oxygen species levels

The positive control group underwent a 2 h pretreatment with 250 μM H_2O_2 to simulate intracellular oxidative stress conditions. Subsequently, cells in this group were administered the test drug. Upon completion of drug administration, the DCFH-DA probe was diluted in serum-free culture medium to a final concentration of 10 μM (1:1000 dilution) and immediately added to the cells, ensuring complete coverage. A subset of probe-treated cells served as the positive control, to which additional H_2O_2 was added to induce oxidative stress. The culture plate was then incubated at 37°C for 30 min, with gentle inversion every 3-5 min to promote uniform probe distribution. Following incubation, cells were washed three times with serum-free medium to remove extracellular DCFH-DA. Fluorescence microscopy (Keyence BZ-H4XD microscope, Keyence Co.) was performed using a 10× eyepiece and 20× objective lens to assess fluorescence intensity and cellular reactive oxygen species (ROS) distribution (Ex: 470/40 nm, Em: 520/50 nm). Random fields were systematically selected, imaged, and documented. Fluorescence intensity was quantified using ImageJ software, with the control group's mean fluorescence intensity set as the baseline (unit 1). All experimental values were normalized to this baseline, yielding relative fluorescence intensities for statistical analysis. To ensure reproducibility, all procedures were performed in triplicate.

ELISA assay

Cells in the logarithmic growth phase were seeded into a 6-well plate at a density of 1×10^6 cells per well. After confirming cell adhesion to the plate surface, experimental treatments were applied according to predefined groupings. Following the intervention, the culture supernatant was carefully aspirated, centrifuged at 1,000 g for 20 min, and the resulting supernatant was collected for downstream analysis as specified by the respective assay kit protocols. Standard samples were prepared in a 96-well plate by serial dilution following the ELISA kit instructions. Each well received 50 μL of standard or test sample, followed by gentle mixing. The plate was sealed and incubated at 37°C for 30 min. The concentrated washing buffer was diluted 30-fold before use. After removing the seal, the plate contents were discarded, and wells were rinsed by filling with diluted washing buffer,

Table 2. Experimental grouping for part 2.

Grouping	Specific procedures
miR-6739-5p mimics+H_2O_2	Treating cells with 250 μmol/L after overexpression of miR-6739-5p in cells
NC mimics+H_2O_2	Control treatment of miR-6739-5p mimics + H_2O_2 group
miR-6739-5p inhibitor+H_2O_2	Treatment of cells with 250 μmol/L after knocking down miR-6739-5p in the cells
miR-6739-5p inhibitor+LY294002+H_2O_2	Cells were treated with 40 μM LY294002 for 4 h after knocking down miR-6739-5p, followed by treatment with 250 μM $H_2O_2$for 2 h
NC inhibitor+H_2O_2	Control treatment group of miR-6739-5p inhibitor + H_2O_2

Table 3. Site information.

Mutation sites	
PI3K3CA 3' UTR	5'-AGAAUUUAUUAGGAGUUUCCCAA-3'
miR-6739-	3'-AUGAACAAGAAAGAGAAAGGGU-5'
MUT PI3K3CA 3' UTR	5'-AGAAUUUAUUAGGAGCTGGGTAA-3'

Table 4. Experimental grouping for part 3.

Grouping	Specific procedures
SSCs	Normal culturing
SSCs+H_2O_2	Cells treated with 250 μmol/L H_2O_2 for 2 h
SSCs+GLEX+H_2O_2	Cells pre-treated with 16 mg/mL GLEX for 12 h followed by treatment with 250 μmol/L H_2O_2 for 2 h
SSCs+740 Y-P+H_2O_2	Cells treated with 20 μM 740 Y-P for 24 h followed by treatment with 250 μmol/L H_2O_2 for 2 h
SSCs+GLEX+ LY294002+H_2O_2	Cells pretreated with 16 mg/mL GLEX for 12 h followed by treatment with 40 μM LY294002 for 4 h and then exposed to 250 μmol/L H_2O_2 for 2 h

shaking off excess liquid, and allowing the plate to stand for 30 s before aspiration. This washing procedure was repeated five times. Next, 50 µL of enzyme-conjugated reagent was added to each well, the plate was resealed, and incubated at 37°C for an additional 30 min. The washing steps were then repeated. Subsequently, 50 µL each of chromogenic substrates A and B were added sequentially to each well, followed by gentle mixing and incubation at 37°C in the dark for 15 min.

Following reaction termination, the optical density (OD) values of each well were measured sequentially at 450 nm to quantify 8-hydroxydeoxyguanosine (8-OHdG), interleukin-1β (IL-1β), and tumor necrosis factor-α (TNF-α). 8-OHdG is a well-established biomarker of DNA oxidative damage, resulting from hydroxyl radical-mediated attack on the guanine base in DNA.[17] Urinary 8-OHdG levels serve as a reliable indicator of systemic oxidative stress, and the enzyme-linked immunosorbent assay (ELISA)-based detection method has been standardized for this purpose.[18] To ensure experimental reproducibility, all procedures were performed in triplicate.

Detection and evaluation of apoptotic cells

Cells in the logarithmic growth phase were seeded at a density of 1×10^6 cells per well in a 6-well plate and assigned to experimental groups accordingly. The cells were cultured in a humidified incubator at 37°C with 5% CO_2 for 24 h. Following incubation, the cells were detached, transferred to centrifuge tubes, and centrifuged at 1,000 rpm for 5 min with an appropriate volume of culture medium. The supernatant was discarded, and the cell pellet was resuspended in 1 mL of PBS, followed by a second centrifugation (1,000 rpm, 5 min) and supernatant removal. This washing step was repeated once. The cell pellet was then resuspended in pre-prepared 1× Annexin V Binding Buffer to achieve a final concentration of 1×10^6 cells/mL. A 100 µL aliquot of the cell suspension was transferred to a fresh tube, and 5 µL each of Annexin V-FITC conjugate and propidium iodide (PI) solution were added. After incubation in the dark at room temperature for 15 min, 400 µL of 1× Annexin V Binding Buffer was added, and the samples were analyzed by flow cytometry (Thermo Fisher Scientific) within 1 h. A total of 1×10^4 events were recorded using a flow cytometer (excitation: 488 nm), and the experimental procedure was performed in triplicate to ensure reproducibility.

Western blot

Cells were seeded in 6-well plates at a density of 1×10^6 cells per well and assigned to experimental groups accordingly. Following a 24-h incubation at 37°C in a humidified atmosphere containing 5% CO_2, the culture supernatant was carefully aspirated. The cell monolayers were then washed twice with pre-chilled PBS. Subsequently, the cells were lysed in 0.5 mL of RIPA lysis buffer supplemented with PMSF. The lysates were clarified by centrifugation at 12,000 g for 5 min at 4°C, and the resulting supernatants (designated as cell protein extracts) were stored at -80°C. Protein concentrations were determined using a BCA protein assay kit. For Western blotting, protein samples were prepared by denaturation in 5× Laemmli loading buffer through boiling for 10 min. SDS-PAGE was performed using a 12% resolving gel and a 5% stacking gel. After electrophoresis, proteins were transferred to PVDF membranes, which were then blocked, incubated with primary and secondary antibodies, and washed thoroughly. Chemiluminescent detection was performed by incubating the membranes with ECL reagents A and B, followed by exposure to X-ray film or digital imaging. The OD of protein bands was quantified using ImageJ software (National Institute of Health, Bethesda, MD, USA), and relative protein expression levels were normalized to internal controls. All experiments were performed in triplicate to ensure reproducibility.

RT-qPCR

Cells were seeded into 6-well plates at a density of 1×10^6 cells per well and assigned to experimental groups accordingly. Following a 24-h incubation at 37°C in a humidified atmosphere containing 5% CO_2, cells were lysed using Buffer RL. The lysates were then processed using FastPure gDNA-Filer Columns III to remove genomic DNA contamination. Ethanol was added to the flow-through, and the mixture was transferred to FastPure RNA Columns III for RNA purification, including binding, washing, and elution steps. RNA bound to the columns was eluted with RNase-free double-distilled water (ddH_2O). The concentration and purity of the RNA were assessed using a spectrophotometer (*e.g.*, NanoDrop). For reverse transcription, 500 ng of RNA was combined with the required reagents in a 200 µL microcentrifuge tube and incubated at 42°C for 2 min to synthesize cDNA. The cDNA was stored at -20°C or -80°C until further use. RT-qPCR was performed using a 20 µL reaction mixture containing 5-fold diluted cDNA, Master Mix, and gene-specific primers. The reactions were run on a real-time fluorescence RT-qPCR instrument under standard cycling conditions. Relative gene expression levels were calculated using the $2^{-\Delta\Delta Ct}$ method, with primer sequences provided in Table 5. All experiments were performed in triplicate to ensure reproducibility.

Fluorescence reporter assay

We initially designed a miR-6739-5p/*PIK3CA* luciferase reporter vector based on the sequence retrieved from the NCBI database and constructed a dual-luciferase reporter plasmid. The plasmids were categorized into five groups: the wild-type control group, the wild-type experimental group, the mutant control group, the mutant experimental group, and the internal reference group. The mutation sites were situated within the 3' untranslated region (3' UTR) of *PIK3CA* and the miR-6739-5p sequence. Consequently, the sequences of the mutant plasmids were modified accordingly. Subsequently, the plasmids carrying the target genes and the internal reference genes were co-transfected into cells at a pre-determined ratio and incubated for 48 h. Upon finishing the plasmid transfection process, we utilized fluorescence microscopy observation to validate the transfection efficiency. More precisely, at designated time intervals following transfection (24 h and 48 h post-transfection), we employed a fluorescence microscope outfitted with suitable excitation and emission filters to examine the expression of fluorescent proteins within the cells, enabling us to conduct an initial evaluation of the transfection efficiency. After finalizing the experimental parameters, we lysed the cells that had been successfully co-transfected and collected the supernatant for the measurement of luciferase activity. The measurement process began with lysing the cells using the Firefly luciferase assay reagent. Samples were then added, and the Firefly luciferase units (Flu values) were measured. This was followed by the addition of the Renilla luciferase assay reagent, after which the Renilla luciferase activity values were calculated. Finally, the relative luciferase activity (RLU) was determined based on the Flu values and RLU values of each group.

MTT experiments

Cells in the logarithmic growth phase were harvested and adjusted to a density of 5,000 cells per well in a 96-well plate by dispensing 100 µL of the cell suspension into each well. The plates were incubated to allow cell attachment, which typically required 8 h. After confirming adherence, the GLEX extract was

diluted in culture medium to final concentrations of 0.25, 0.5, 1.0, 2.0, 4.0, 8.0, and 16.0 mg/mL. Each concentration was applied to the cells and incubated for 24 h. Cell viability was assessed using the MTT assay. Briefly, 10 µL of MTT staining solution was added to each well, followed by a 4-h incubation. Subsequently, 100 µL of formazan-dissolving solution was added to each well and mixed gently to ensure complete dissolution of formazan crystals. The plates were incubated for an additional 3-4 h to stabilize color development. Absorbance at 570 nm was measured using a microplate reader, and cell viability (%) was calculated as: [(mean absorbance of the experimental group − mean absorbance of the blank group) / (mean absorbance of the control group − mean absorbance of the blank group)] × 100%. All experiments were performed in triplicate to ensure reproducibility and accuracy.

Statistical analysis

Statistical analyses and data visualization were performed using GraphPad Prism 9 (Version 9.5.1; La Jolla, CA, USA) and ImageJ software. Data organization and figure assembly were conducted with Adobe Illustrator (2023). All data are presented as means SD, with error bars representing SD values. For pairwise comparisons, an unpaired Student's *t*-test was used, while one-way analysis of variance (ANOVA) followed by *post-hoc* tests (*e.g.*, Tukey's or Dunnett's) was applied for multiple comparisons. Statistical significance was defined as $p<0.05$, with asterisks denoting significance levels: $^{*}p<0.05$, $^{**}p<0.01$, $^{***}p<0.001$.

Results

Induction of oxidative stress response in spermatogonial cells by H_2O_2 treatment

As shown in Figure 1, treatment of spermatogonial cells with 250 µmol/L H_2O_2 for 2 h significantly reduced both cell proliferation and viability compared to the control group ($p<0.05$). Concurrently, apoptotic levels in treated cells increased markedly ($p<0.05$). Furthermore, this oxidative stress induction elevated intracellular ROS accumulation and DNA oxidative damage ($p<0.05$). These collective findings indicate that a 2 h exposure to 250 µmol/L H_2O_2 triggers oxidative stress responses in spermatogonial cells.

H_2O_2 treatment increases the expression level of miR-6739-5p in spermatogonial cells

To investigate the potential role of miR-6739-5p in H_2O_2-induced functional alterations in spermatogonial cells, we examined miR-6739-5p expression levels following H_2O_2 treatment. Our results demonstrated that H_2O_2 exposure significantly upregulated miR-6739-5p abundance in spermatogonial cells. Furthermore, H_2O_2 treatment substantially downregulated the expression of *PIK3CA*, p-PI3K, and p-AKT in these cells (Figure 2). Collectively, these findings suggest that miR-6739-5p may serve as a key mediator in H_2O_2-induced functional changes in spermatogonial cells, potentially *via* modulation of the PI3K/AKT signaling pathway.

miR-6739-5p modulates oxidative stress damage in spermatogonial cells *via* the PI3K/AKT pathway

As shown in Figure 3, overexpression of miR-6739-5p potentiated H_2O_2-induced cytotoxicity in spermatogonial cells, exacerbating reductions in cell viability, elevations in ROS levels, and downregulation of *PIK3CA*, p-PI3K, and p-AKT expression (all $p<0.05$). Conversely, miR-6739-5p knockdown significantly attenuated these adverse effects ($p<0.05$). Notably, combined treatment with a PI3K/AKT inhibitor in miR-6739-5p-knockdown cells further decreased cell viability and increased ROS accumulation compared to miR-6739-5p knockdown alone. Dual-luciferase reporter assays confirmed direct targeting of *PIK3CA* by miR-6739-5p. Collectively, these findings demonstrate that miR-6739-5p regulates the PI3K/AKT pathway to modulate oxidative stress responses in spermatogonial cells.

Treatment with GLEX significantly enhances viability of spermatogonial cells

As depicted in Figure 4, GLEX exhibited no cytotoxicity toward spermatogonial cells across concentrations of 0-16 mg/mL, as confirmed by non-significant differences ($p>0.05$). Consequently, 16 mg/mL GLEX was selected for subsequent experiments. Pre-treatment with GLEX for 12 h significantly attenuated H_2O_2-induced cellular damage, restoring cell viability, enhancing proliferative capacity, and reducing apoptosis levels (all $p<0.05$). Notably, GLEX demonstrated comparable efficacy to a PI3K/AKT pathway activator, with no significant differences observed between treatments ($p>0.05$). These findings underscore the therapeutic potential of GLEX in mitigating H_2O_2-induced spermatogonial cell dysfunction.

GLEX regulates the activation of the PI3K/AKT pathway through downregulating miR-6739-5p

As shown in Figure 5, 12-h GLEX pre-treatment of spermatogonial cells effectively alleviated H_2O_2-induced oxidative stress and inflammation, evidenced by significant reductions in intracellular ROS, 8-OHdG, TNF-α, and IL-1β levels (all $p<0.05$). Notably, GLEX pre-treatment concurrently downregulated miR-6739-5p expression while upregulating *PIK3CA*, p-PI3K, p-AKT, and Nrf2. These effects were comparable to those of a PI3K/AKT pathway activator, with no significant differences between treatments ($p>0.05$). When integrated with our prior findings, these results strongly indicate that GLEX modulates PI3K/AKT pathway activation through miR-6739-5p downregulation.

Table 5. Primer information.

Gene	Primer sequence (5' to 3')
hsa-miR-6739-5p	Forward: TCGGCAGGTGGGAAAG Reverse: CTCAACTGGTGTCGTGGA
U6	Forward: GCTTCGGCAGCACATATACTAAAAT Reverse: CGCTTCACGAATTTGCGTGTCAT

Discussion

The present study conducted a comprehensive investigation into the mechanisms by which GLEX mitigates H_2O_2-induced oxidative damage in spermatogonial cells, with particular focus on elucidating the regulatory roles of miR-6739-5p and the PI3K/AKT signaling pathway. Through a rigorously designed experimental approach and multi-dimensional analyses, we demonstrated that GLEX activates the PI3K/AKT pathway *via* downregulation of miR-6739-5p, thereby significantly attenuating oxidative stress-mediated cellular injury in spermatogonia.

Oxidative stress, characterized by excessive ROS attacking cells, has long been recognized as a major contributor to male infertility, as supported by numerous studies.[19,20] Elevated ROS levels induce DNA damage, mitochondrial dysfunction, and lipid peroxidation in spermatogonial cells, thereby disrupting spermatogenesis and impairing sperm function.[21,22] In this study, we successfully established an oxidative stress model by exposing spermatogonial cells to 250 μmol/L H_2O_2 for 2 h, which significantly inhibited cell proliferation and viability while increasing

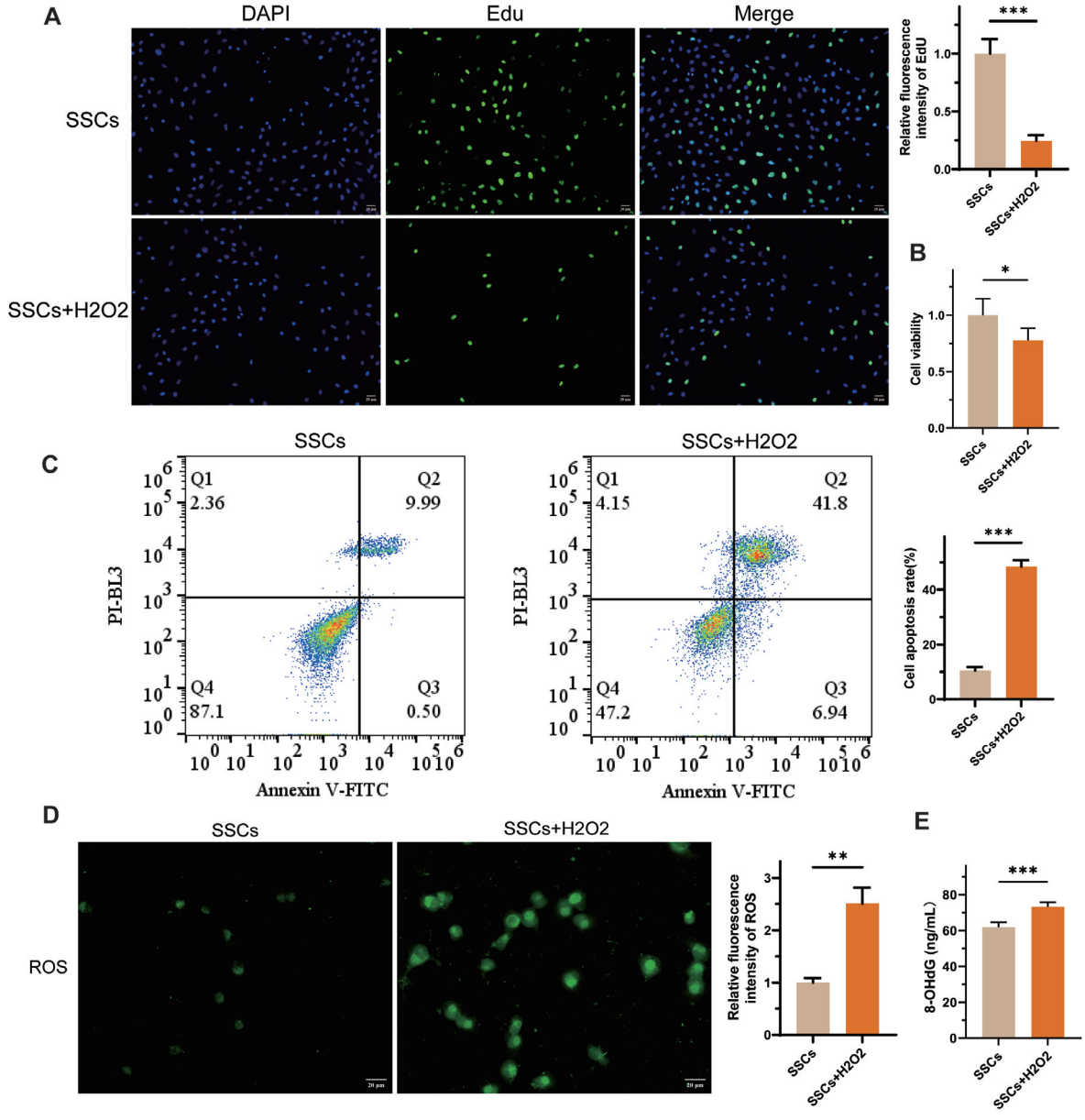

Figure 1. Induction of oxidative stress response in spermatogonial cells by H_2O_2 treatment. **A**) Changes in cell proliferation was determined by EdU assay; DAPI: Ex:358, Em:461; EdU: Ex:495, Em:519; scale bar: 20 μm. **B**) Variation in cell viability was determined by CCK-8 assay. **C**) Apoptosis status of cells was determined by flow cytometry. **D**) Alteration in ROS level was determined by ROS measuring kits; Ex: 470/40, Em: 520/50; scale bar: 20 μm. **E**) 8-OHdG level was determined by ELISA kits. n=3; *p<0.05, **p<0.01, ***p<0.001.

apoptosis rates, ROS levels, and DNA damage. These findings align with previous research[23], reinforcing the critical role of oxidative stress in spermatogonial cell injury.

miRNAs represent essential regulators of gene expression with significant implications in the reproductive system. Extensive evidence demonstrates their abundant presence in male reproductive tissues, including the testis, epididymis, spermatozoa, seminal plasma, and extracellular vesicles such as exosomes.[24,25] Dysregulated miRNA expression can alter spermatogenesis and embryo development, potentially underlying various forms of infertility. For instance, miR-6739-5p is significantly upregulated in patients with oligoasthenozoospermia,[9] suggesting its involvement in male infertility pathogenesis. Our study confirmed that H_2O_2 treatment substantially increased miR-6739-5p expression in spermatogonial cells. Functional experiments revealed that miR-6739-5p overexpression exacerbated H_2O_2-induced cell damage, whereas its knockdown mitigated such damage, indicating its potential as a therapeutic target for oligoasthenozoospermia. Additionally, miR-21-5p regulates cellular development and differentiation processes, influencing cell proliferation, energy metabolism, and male reproductive function.[26]

The PI3K/AKT signaling pathway plays a pivotal role in regulating cell survival, proliferation, and metabolism.[2]. with critical functions in spermatogenesis and sperm function maintenance. Previous studies demonstrated that this pathway enhances proliferation and anti-apoptotic capacity in immature Sertoli and spermatogenic cells.[28] Our study provides compelling evidence that miR-6739-5p modulates oxidative stress responses in spermatogonial cells by suppressing PI3K/AKT pathway activity. Specifically, miR-6739-5p overexpression decreased *PIK3CA*, p-PI3K, and p-AKT levels, aggravating H_2O_2-induced damage. Conversely, miR-6739-5p knockdown restored PI3K/AKT pathway activity and improved cell survival, effects confirmed by dual-luciferase reporter assays and pathway inhibitor treatments.

TCM offers unique advantages in treating refractory diseases, including facial paralysis, asthma, inflammatory disorders, and cancers[29-31] with demonstrated efficacy in oligoasthenozoospermia management.[32] GLEX, a TCM herbal formula with a long history of treating male reproductive disorders,[15] was investigated for its protective mechanisms against oxidative stress. Our results showed that GLEX (0-16 mg/mL) exhibited no cytotoxicity in spermatogonial cells. Pre-treatment with 12 mg/mL GLEX for 12 h significantly attenuated H_2O_2-induced damage, restoring cell viability and proliferation while reducing apoptosis. Mechanistically, GLEX downregulated miR-6739-5p expression and activated the PI3K/AKT pathway, thereby decreasing oxidative stress markers (ROS, 8-OHdG) and inflammatory factors (TNF-α, IL-1β). These findings suggest that GLEX protects spermatogonial cells by activating PI3K/AKT signaling through miR-6739-5p modulation, thereby alleviating oxidative stress-induced injury. This study elucidates the mechanism underlying GLEX's therapeutic effects in male infertility, demonstrating its ability to mitigate oxidative stress damage by regulating miR-6739-5p and the PI3K/AKT pathway, thereby enhancing spermatogonial cell function. These findings provide a theoretical

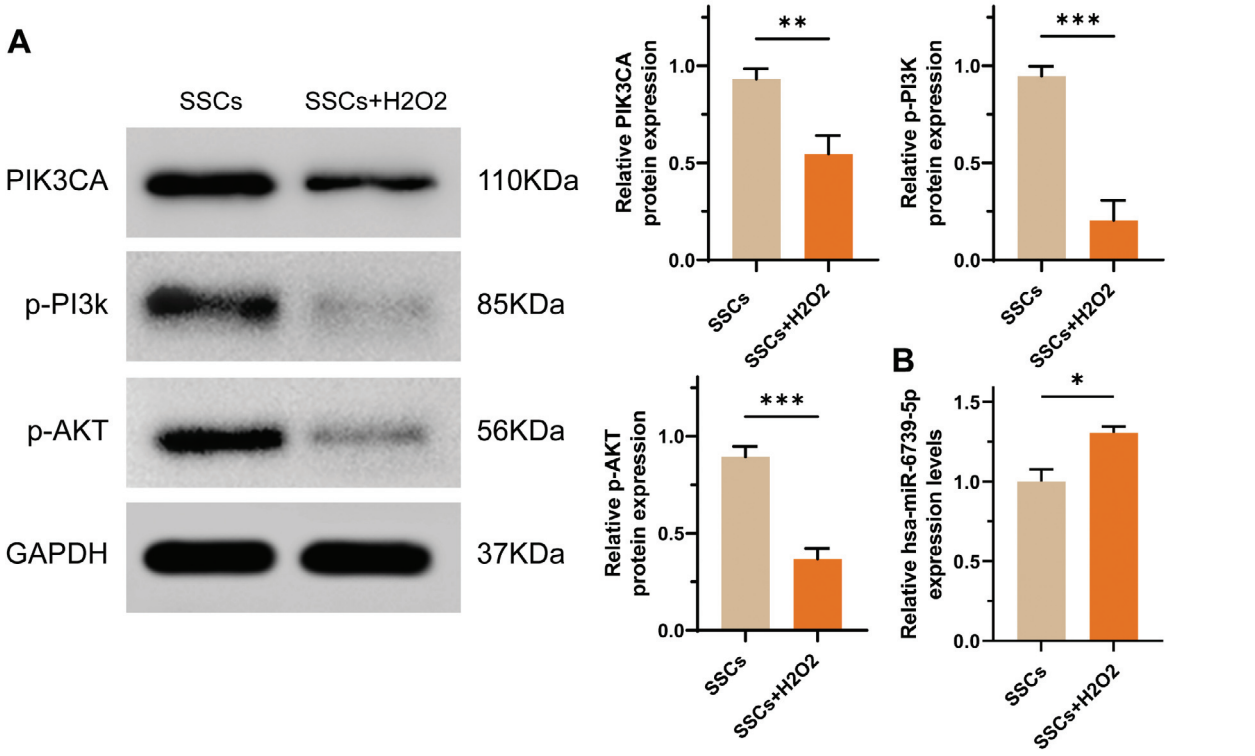

Figure 2. Potential mechanisms of H_2O_2-induced changes in spermatogonial cell viability. **A**) Expression levels of PIK3CA, p-PI3K, and p-AKT after H_2O_2 treatment were determined by Western blotting assay. **B**) Changes in miR-6739-5p levels following H_2O_2 treatment were determined by RT-qPCR. n=3; *p<0.05, **p<0.01, ***p<0.001.

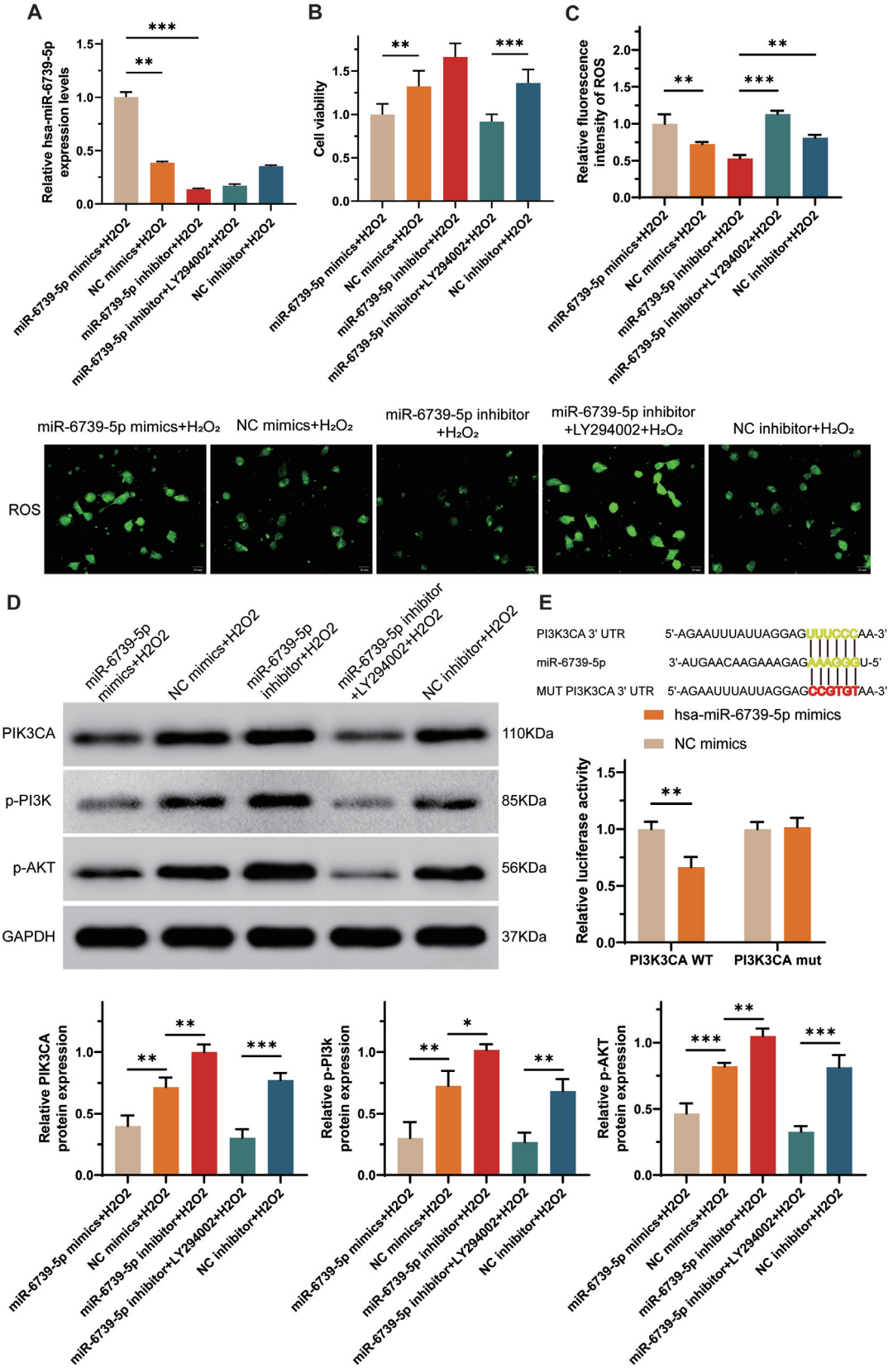

Figure 3. miR-6739-5p modulates oxidative stress damage in spermatogonial cells *via* the PI3K/AKT pathway. **A**) Expression levels of miR-6739-5p were determined by RT-qPCR. **B**) Viability of spermatogonial cells in different treatment groups were determined by CCK8 assays. **C**) Levels of ROS in spermatogonial cells in different treatment groups were determined by ROS measuring kits; Ex: 470/40, Em: 520/50; scale bar: 20 μm. **D**) Expression levels of PIK3CA, p-PI3K, and p-AKT in spermatogonial cells in different treatment groups were determined by Western blotting assay. E) The targeting effect of miR-6739-5p and PI3KCA was evaluated by dual-luciferase reporter assay. n=3; **p*<0.05, ***p*<0.01, ****p*<0.001.

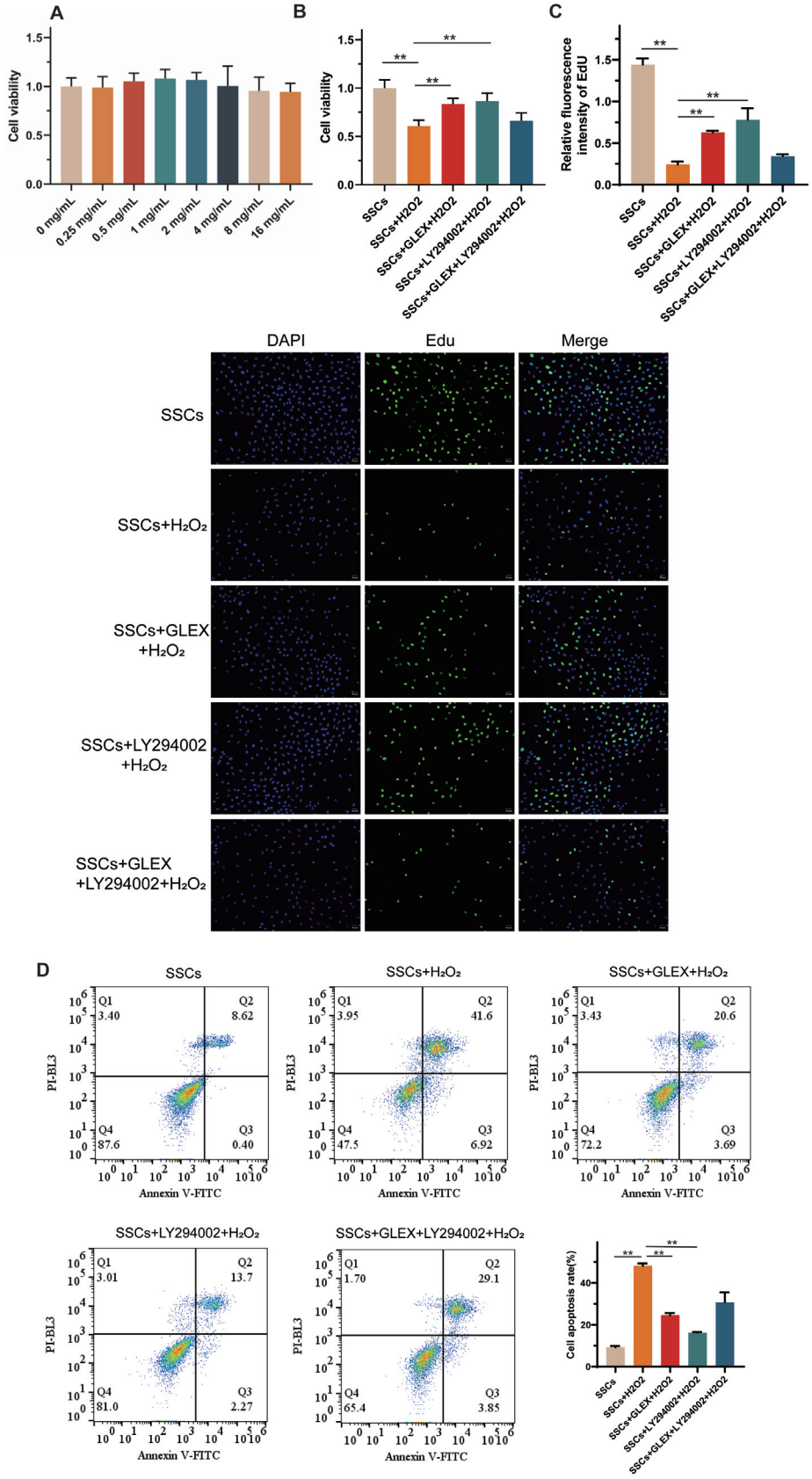

Figure 4. GLEX enhances viability of spermatogonial cells. **A**) Cell toxicity was measured by MTT assay. **B**) Changes in cell viability with different treatments were determined by CCK-8 assay. **C**) Changes in proliferative capacity of cells with different treatments were determined by EdU assay; DAPI: Ex:358, Em:461; EdU: Ex:495, Em:519; scale bar: 20 μm. **D**) Apoptosis levels in cells with different treatments were determined by flow cytometry. n=3; *p<0.05, **p<0.01, ***p<0.001.

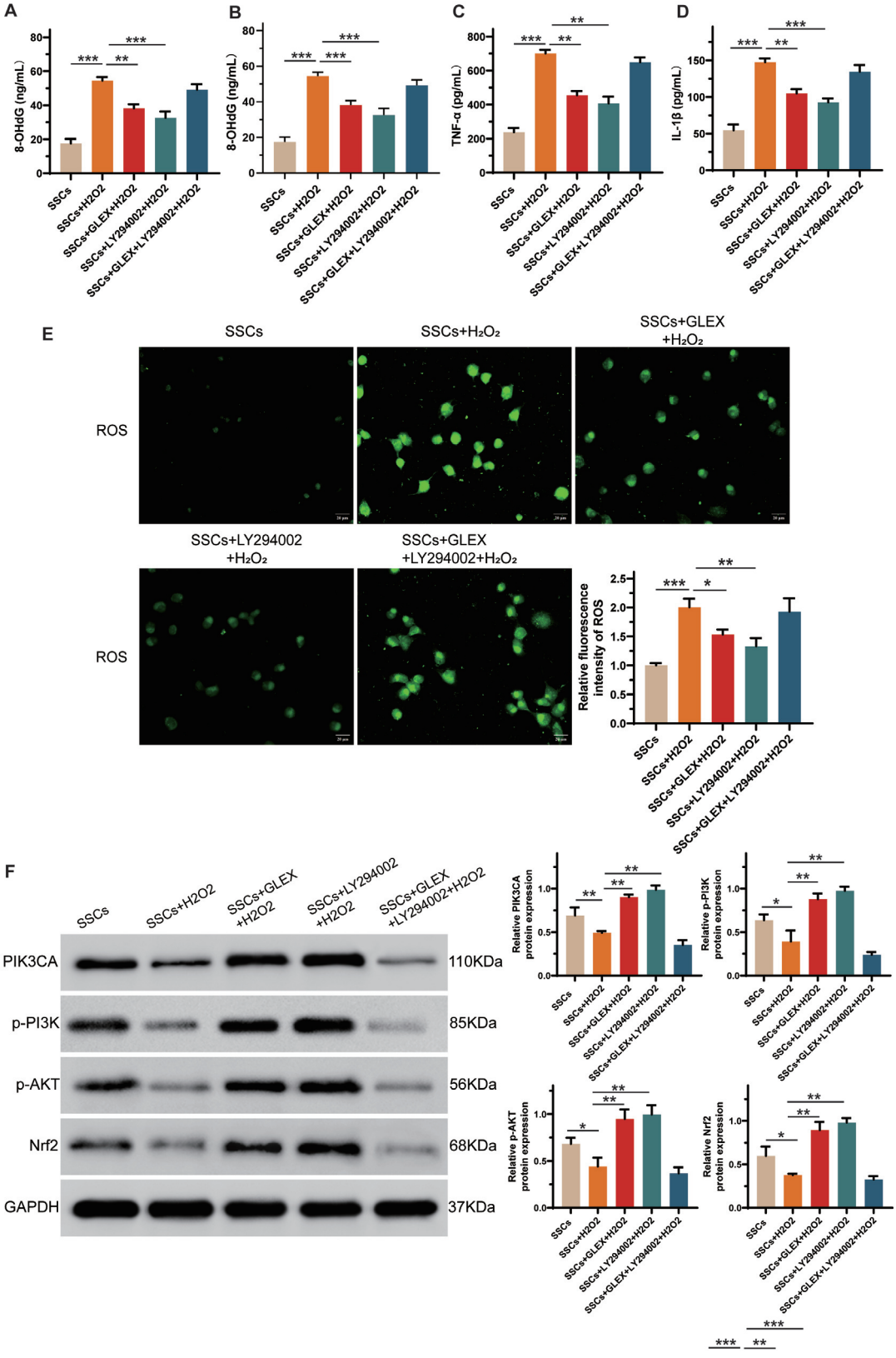

Figure 5. GLEX regulates the activation of the PI3K/AKT pathway through miR-6739-5p. **A**) Changes in 8-OHdG levels with different treatments were measured by ELISA kits. **B**) Expression levels of TNF-α with different treatments were measured by ELISA kits. **C**) Expression levels of IL-1β with different treatments were measured by ELISA kits. D) Expression levels of miR-6739-5p with different treatments were determined by RT-qPCR. **E**) Changes in ROS levels with different treatments were observed by ROS measuring kits; scale bar: 20 μm. **F**) Expression levels of *PIK3CA*, p-PI3K, p-AKT, and Nrf2 with different treatments were determined by Western blotting. n=3; **p*<0.05, ***p*<0.01, ****p*<0.001.

foundation for developing novel infertility treatments. However, limitations exist: the active components of GLEX remain unidentified, and its *in vivo* metabolism and pharmacokinetics require further investigation. Additionally, long-term safety and clinical efficacy warrant rigorous evaluation. Given TCM's holistic properties and traditional usage, we hypothesize that GLEX may confer *in vivo* protection by improving the testicular microenvironment, modulating reproductive hormone secretion, and suppressing oxidative stress. Nevertheless, due to male infertility's heterogeneous etiology and the limitations of cell models in replicating testicular physiology, animal studies are essential for validating pharmacological mechanisms and optimizing clinical applications.

In conclusion, this study systematically reveals the mechanism by which GLEX protects spermatogonial cells from oxidative stress through miR-6739-5p and PI3K/AKT pathway regulation, offering new insights for male infertility treatment. Future research should focus on clinical translation and mechanistic refinement to improve male reproductive health outcomes.

References

1. Lundy SD, Sangwan N, Parekh NV, Selvam M, Gupta S, McCaffrey P, et al. Functional and taxonomic dysbiosis of the gut, urine, and semen microbiomes in male Infertility. Eur Urol 2021;79:826-36.
2. Agarwal A, Baskaran S, Parekh N, Cho CL, Henkel R, Vij S, et al. Male infertility. Lancet 2021;397:319-33.
3. Bisht S, Faiq M, Tolahunase M, Dada R. Oxidative stress and male infertility. Nat Rev Urol 2017;14:470-85.
4. Aitken RJ, Drevet JR, Moazamian A, Gharagozloo P. Male infertility and oxidative stress: a focus on the underlying mechanisms. Antioxidants (Basel) 2022;11:306.
5. Jungwirth A, Giwercman A, Tournaye H, Diemer T, Kopa Z, Dohle G, et al. European Association of Urology guidelines on male infertility: the 2012 update. Eur Urol 2012;62:324-32.
6. Krausz C, Escamilla AR, Chianese C. Genetics of male infertility: from research to clinic. Reproduction 2015;150:R159-74.
7. Liang Y, Ridzon D, Wong L, Chen C. Characterization of microRNA expression profiles in normal human tissues. Bmc Genomics 2007;8:166.
8. Forouhari S, Mahmoudi E, Safdarian E, Beygi Z, Gheibihayat SM. MicroRNA: a potential diagnosis for male infertility. Mini Rev Med Chem 2021;21:1226-36.
9. Liang G, Wang Q, Zhang G, Li Z, Wang Q. Differentially expressed miRNAs and potential therapeutic targets for asthenospermia. Andrologia 2022;54:e14265.
10. Xu CL, Tan QY, Yang H, Li CY, Wu Z, Ma YF. Melatonin enhances spermatogonia activity through promoting KIAA1429-mediated m(6)A deposition to activate the PI3K/AKT signaling. Reprod Biol 2022;22:100681.
11. Cannarella R, Petralia CMB, Condorelli RA, Aversa A, Calogero AE, La Vignera S. Investigational follicle-stimulating hormone receptor agonists for male infertility therapy. Expert Opin Investig Drugs 2023;32:813-824.
12. Yang B, Meng QY, Chen H, Gao YL, Shen J, Mu YY, et al. [Clinical effect of acupuncture combined with traditional Chinese medicine in treatment of oligozoospermia/asthenozoospermia: a meta-analysis].[Article in Chinese]. Zhen Ci Yan Jiu 2020;45:243-50.
13. Zhao MP, Shi X, Kong G, Wang CC, Wu J, Lin ZX, et al. The therapeutic effects of a traditional Chinese medicine formula Wuzi Yanzong pill for the treatment of oligoasthenozoospermia: a meta-analysis of randomized controlled trials. Evid Based Complement Alternat Med 2018;2018:2968025.
14. Ren J. Clinical study on the treatment of oligoasthenozoospermia with kidney deficiency syndrome by Guilu Erxian Paste. Master's thesis, Hunan University of Chinese Medicine. 2023.
15. Ding J, Lu B, Liu L, Zhong Z, Wang N, Li B, et al. Guilu-Erxian-Glue alleviates Tripterygium wilfordii polyglycoside-induced oligoasthenospermia in rats by resisting ferroptosis via the Keap1/Nrf2/GPX4 signaling pathway. Pharm Biol 2023;61:213-27.
16. Wang H, Li C, Zhu L, Liu Z, Li N, Zheng Z, et al. Adiponectin attenuates H2O2-induced apoptosis in chicken skeletal myoblasts through the lysosomal-mitochondrial axis. In Vitro Cell Dev Biol Anim 2024;60:805-14.
17. Vorilhon S, Brugnon F, Kocer A, Dollet S, Bourgne C, Berger M, et al. Accuracy of human sperm DNA oxidation quantification and threshold determination using an 8-OHdG immunodetection assay. Hum Reprod 2018;33:553-62.
18. Graille M, Wild P, Sauvain JJ, Hemmendinger M, Guseva Canu I, Hopf NB. Urinary 8-OHdG as a biomarker for oxidative stress: a systematic literature review and meta-analysis. Int J Mol Sci 2020;21:3743.
19. Sies H, Berndt C, Jones DP. Oxidative stress. Annu Rev Biochem 2017;86:715-48.
20. Hussain T, Kandeel M, Metwally E, Murtaza G, Kalhoro DH, Yin Y, et al. Unraveling the harmful effect of oxidative stress on male fertility: A mechanistic insight. Front Endocrinol (Lausanne) 2023;14:1070692.
21. Pena FJ, O'Flaherty C, Ortiz RJ, Martin CF, Gaitskell-Phillips GL, Gil MC, et al. Redox regulation and oxidative stress: the particular case of the stallion spermatozoa. Antioxidants (Basel) 2019;8:567.
22. Ferrer MS, Palomares R, Hurley D, Bullington AC, Hoyos-Jaramillo A, Bittar JH. Antisperm antibodies and sperm function in bulls undergoing scrotal insulation. Reproduction 2020;160:783-92.
23. Bromfield EG, Aitken RJ, McLaughlin EA, Nixon B. Proteolytic degradation of heat shock protein A2 occurs in response to oxidative stress in male germ cells of the mouse. Mol Hum Reprod 2017;23:91-105.
24. Salas-Huetos A, James ER, Aston KI, Carrell DT, Jenkins TG, Yeste M. The role of miRNAs in male human reproduction: a systematic review. Andrology 2020;8:7-26.
25. Salilew-Wondim D, Gebremedhn S, Hoelker M, Tholen E, Hailay T, Tesfaye D. The role of microRNAs in mammalian fertility: from gametogenesis to embryo implantation. Int J Mol Sci 2020;21:585.
26. Yang CX, Yang YW, Mou Q, Chen L, Huo LJ, Du ZQ. Global alteration of microRNA expression induced by vitamin C treatment in immature boar Sertoli cells. Theriogenology 2022;183:1-9.
27. Cai B, Zheng Y, Ma S, Xing Q, Wang X, Yang B, et al. Long non−coding RNA regulates hair follicle stem cell proliferation and differentiation through PI3K/AKT signal pathway. Mol Med Rep 2018;17:5477-83.
28. Chen KQ, Wei BH, Hao SL, Yang WX. The PI3K/AKT signaling pathway: How does it regulate development of Sertoli cells and spermatogenic cells? Histol Histopathol 2022;37:621-36.
29. Zhou Y, Dong X, Xing Y, Wang R, Yang S, Han Y, Wang D. Effects of electroacupuncture therapy on intractable facial paralysis: A systematic review and meta-analysis. PLoS One 2023;18:e0288606.
30. Song W, Zheng S, Li M, Zhang X, Cao R, Ye C, et al. Linking endotypes to omics profiles in difficult-to-control asthma using the diagnostic Chinese medicine syndrome differentiation

algorithm. J Asthma 2020;57:532-42.
31. Li D, Xu KY, Zhao WP, Liu MF, Feng R, Li DQ, et al. Chinese medicinal herb-derived carbon dots for common diseases: efficacies and potential mechanisms. Front Pharmacol 2022;13:815479.
32. Zheng YF, Bai X, Tang YB, Liu GM, Liu D, Fan XL, et al. [Academician Wang Qi's medication rules for oligoasthenozoospermia: An analysis based on the traditional Chinese medicine inheritance auxiliary platform].[Article in Chinese with English abstract]. Zhonghua Nan Ke Xue 2020;26:532-42.

Received: 16 July 2025. Accepted: 4 September 2025.

European Journal of Histochemistry 2025; 69:4253
doi:10.4081/ejh.2025.4253